Jurnal Ilmu Fisika
Vol. 14, No. 2, September 2022, pp. 116–123
ISSN: 1979-4657 (Print); 2614-7386 (Online)
https://doi.org/10.25077/jif.14.2.116-123.2022

Jurnal Ilmu Fisika
Open Access

Photocatalytic Properties of Co-precipitated Bismuth Cobalt Ferrite

Abi Catur Saputri, Nurdiyantoro Putra Prasetya, Utari Utari, Budi Purnama

Department of Physics, Faculty of Mathematics and Natural Sciences, Sebelas Maret University, Surakarta, 57126, Central Java, Indonesia

Article Info

Article History:

Received July 30, 2022
Revised August 14, 2022
Accepted August 27, 2022

Keywords:

nanoparticle
bismuth cobalt ferrite
coprecipitation
photocatalyst

Corresponding Author:

Budi Purnama,
Email: bpurnama@mipa.uns.ac.id

ABSTRACT

Bismuth substituted cobalt ferrite nanoparticle is studied for photocatalytic in this paper. Bismuth cobalt ferrite has been synthesized by the coprecipitation method and low-temperature annealing treatment. The characterization results showed that the XRD spectral pattern is consistent with ICDD 221086. The crystallite size of bismuth cobalt ferrite increases with increasing annealing temperature. FTIR results confirm the available metal–oxide at number wave around 570/cm and 475/cm which is the appearance of octahedral and tetrahedral sites owing cobalt ferrite. The photocatalyst test was carried out by varying the catalyst mass and UV irradiation time. The absorption spectrum decreases with increasing catalyst mass. The increase in UV irradiation time causes the formation of more holes (h^+) and electrons (e^-). So that the hydroxide reaction occurs that produces free radicals. The results of this study indicate that cobalt ferrite-based nanoparticles have potential as photocatalyst materials.

1. INTRODUCTION

In recent years, cobalt ferrite spinel particles ($CoFe_2O_4$) have attracted much interest in research due to their excellent magnetic and electrical properties (Zhou et al., 2015). Cobalt ferrite belongs to the spinel ferrite group with the formula $M^{2+}Fe_2^{3+}O_4$, where M is a divalent ion such as Mn^{2+}, Ni^{2+}, Co^{2+}, Cd^{2+}, Mg^{2+}, Fe^{2+} (Kotnala & Shah, 2015). Cobalt ferrite has an inverse spinel structure in which, in the theoretical viewpoint, all divalent ions are at site B (octahedral) and trivalent ions are distributed evenly between site A (tetrahedral) and site B (octahedral) (Goodarz Naseri et al., 2010). The variations in the distribution of cations open up opportunities to modify the physical properties of cobalt ferrite by doping other cations. Several nanoparticle synthesis methods have been developed, including the coprecipitation method, sol-gel method, hydrothermal method, and glycine nitrate process (Amiri & Shokrollahi, 2013; Hajalilou et al., 2016; Gingasu et al., 2015). Among these methods, the coprecipitation method is the most effective and the simplest (Setiadi et al., 2016). Cobalt ferrite is very easy to prepare and relatively inexpensive, these particles are also very useful in the biomedical field. In the biomedical applications, cobalt ferrite is potentially used as a catalyst, magnetic fluid, and drug delivery material (Ramli et al., 2017).

Several researchers have succeeded in substituting bismuth ions in cobalt ferrite. Research conducted by Routray et al., (2017), shows that the effect of bismuth substitution on cobalt ferrite is to change the crystallite size and reduce saturation magnetization, coercivity, remanent magnetization,

and magnetic moment. The same thing was conveyed by Kapoor et al., (2018), in their research on cobalt ferrite substituted with bismuth ion. The doped product (x = 0.02; x = 0.04 and x = 0.06) has a lower band gap than that of pure cobalt ferrite and shows an increase in the rate of the degradation reaction. By the characteristics that have been reported by several researchers, bismuth cobalt ferrite has potential in photocatalyst applications. Therefore, this study aims to confirm that bismuth cobalt ferrite samples can be used for photocatalyst applications with higher doping concentrations (x = 0.15).

In this study, bismuth cobalt ferrite was synthesized using the coprecipitation method with annealing treatment at temperatures (200 °C, 300 °C, 400 °C, and 500 °C). The annealing temperature treatment is often carried out to control the crystallite size of the material (Arilasita et al., 2020). The annealing treatment also improves the crystallinity and magnetic properties of the material (Amer et al., 2015). Thus, bismuth cobalt ferrite with annealing treatment has potential in photocatalyst applications.

Photocatalysis is the process of combining photoreaction with a catalyst, where the catalyst is a substance that is used to speed up the reaction rate but does not appear after the reaction, thus reducing the activation energy of the reaction. The characteristics of a good or ideal photocatalyst material are that it can be activated by photons, is chemically unreactive, easy to obtain, non-toxic, and able to utilize a broad spectrum of the sun. Light is needed to activate the catalyst so that the photocatalytic reaction can take place. When a photon of sufficient energy (≥ energy gap of the semiconductor catalyst) is absorbed by the catalyst, an electron from the valence band (VB) is excited to the conduction band (CB) and, produces a hole in the VB. The process of forming this electron-hole pair is called photoexcitation (Safaat, 2020).

The sample was characterized using X-Ray Diffractometer (XRD), Fourier Transform Infrared (FTIR), and Vibrating Sample Magnetometer (VSM). Then the sample was applied as a catalyst to degrade the color of organic pollutants or methylene blue. In this study, the mass of bismuth cobalt ferrite catalyst and UV irradiation time were varied.

2. MATERIALS AND METHOD

2.1 Materials

The Materials used are 4.8M NaOH solution, $CoBi_{0.15}Fe_{1.85}O_4$ ($Fe(NO_3)_3.9H_2O$, $Co(NO_3)_2.6H_2O$, and $Bi(NO_3)_3.5H_2O$), aqua-bides (double distilled water), ethanol, and methylene blue 20 ppm.

2.2 Co-Precipitation Method

The coprecipitation synthesis of bismuth cobalt ferrite nanoparticles began with the preparation of 4.8M NaOH solution and $CoBi_{0.15}Fe_{1.85}O_4$ solution (Zhang et al., 2010; Arilasita et al., 2020). Then the titration process was carried out on the sample using NaOH solution. Thereafter the samples were deposited until the solution settled. After settling, the samples were washed using ethanol and distilled water, three times each, and washing was carried out for 10 minutes using a magnetic stirrer. Then the sample was deposited again. Then the sample precipitate was placed into a crucible for the hydrolysis process. The hydrolysis process was carried out to remove the remaining water in the sediment so that the sample can dry. This hydrolysis process uses a Memmert oven at 100 °C for 12 hours. After that, the sample was pounded for one hour in a constant direction. Sample mashing was done to smooth the sample so that it becomes fine granules. The crushed sample then enters the annealing process. This process was carried out using a Brother XD-1400S furnace for five hours and using various temperatures (200 °C, 300 °C, 400 °C, and 500 °C). After the annealing process was completed, the sample was again pounded using a pestle and mortar for two hours. The collision was carried out in a constant direction so that the sample size became more homogeneous.

2.3 UV-Vis Spectrophotometer

The results of the UV-Vis test were plotted using SMA4 software to obtain the relationship between wavelength and absorbance. The degradation of methylene blue dye was calculated using the following equation (Labhane et al., 2015) :

$$\%\ \text{Degradation} = \left(\frac{C_0 - C_t}{C_0}\right) \times 100\% \quad (1)$$

where C_0 is the initial concentration of dye and C_t is the concentration of dye after irradiation time 't'.

The band gap energy (E_g) of nanoparticles can be calculated from the fundamental absorption, which corresponds to the excitation of electrons from the valence band to the conduction band. The optical band gap is calculated from the following equation (Kiran & Sumathi, 2017) :

$$\alpha h\nu = A\left(h\nu - E_g\right)^{1/2} \quad (2)$$

where α is absorption coefficient, h is Plank's constant, v is light frequency, E_g is band gap, and A is proportionality constant. The photocatalytic reaction can be illustrated in Figure 1.

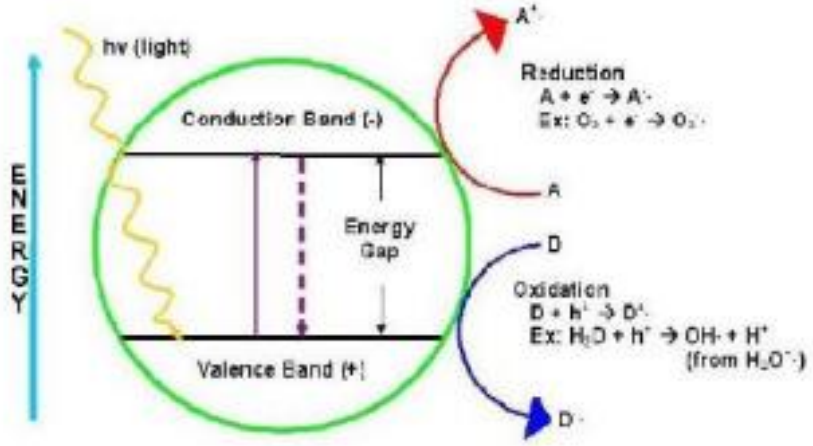

Figure 1 Photochemically excited photocatalyst material process (Syam & Hendri, 2014).

3. RESULTS AND DISCUSSION

3.1 Crystallite Structure Analysis

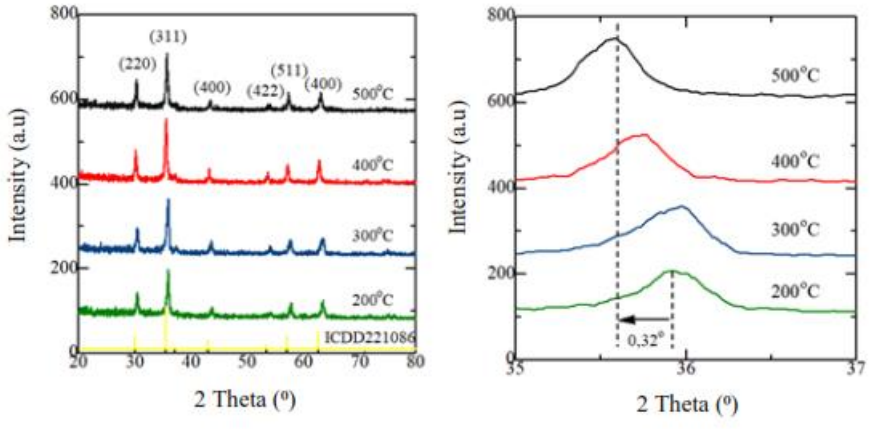

(a) (b)

Figure 2 (a) XRD spectral pattern of bismuth cobalt ferrite sample and (b) Peak at crystallite orientation (311).

The results of the XRD characterization of a sample of cobalt ferrite doped with bismuth using the coprecipitation method and annealing treatment at low temperatures (200 °C, 300 °C, 400 °C, and

500 °C) are shown in Figure 2. The XRD pattern shows the occurrence of the strongest peak shift to a small angle with increasing annealing temperature. These results are in line with the results of a study by Saputro et al., (2019) which revealed that the highest peak angle of the cobalt ferrite sample shifted when the cobalt ferrite was doped with bismuth ion. The XRD spectral pattern shows diffraction peaks in the hkl (220), (311), (400), (511), and (440) planes which are the same as the International Center for Diffraction Data (ICDD) number 221086 which implies the cubic spinel structure with Fd3m space group symmetry (Sundararajan et al., 2017).

3.2 Chemical Bonding Group Analysis

The Fourier Transform Infrared (FTIR) spectrum pattern of $CoBi_{0.15}Fe_{1.85}O_4$ the sample is shown in Figure 3. This FTIR characterization was used to identify the oxide bond of $CoBi_{0.15}Fe_{1.85}O_4$ sample. Samples were measured and observed at wave numbers 400 – 4000 cm^{-1}.

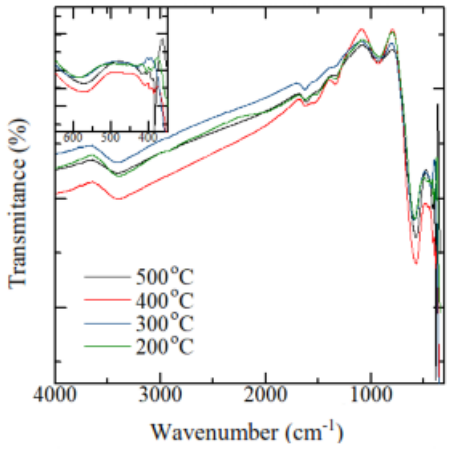

Figure 3 FTIR spectrum of bismuth cobalt ferrite samples annealed at different temperatures.

The results of this FTIR characterization showed that the annealing treatment at low temperatures (200 °C, 300 °C, 400 °C, and 500 °C) produced different spectral patterns. In this FTIR spectrum pattern, there is an absorption curve in the range of wave number (600 – 400) cm^{-1} caused by the stretching vibrations of metal ions in octahedral and tetrahedral sites (Sumathi & Lakshmipriya, 2017). It is alleged that the annealing treatment of $CoBi_{0.15}Fe_{1.85}O_4$ sample resulted in an increase in the redistribution of cations at the tetrahedral and octahedral sites.

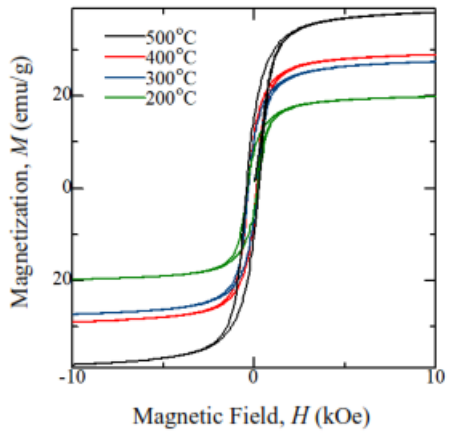

Figure 4 Hysteresis curve of bismuth cobalt ferrite samples annealed at different temperatures.

3.3 Magnetic Properties Analysis

The hysteresis curve of the $CoBi_{0.15}Fe_{1.85}O_4$ sample with variations in annealing temperature is shown in Figure 4. The treatment of variations in annealing temperature can affect the magnetic properties of the sample as indicated by changes in the width, height, and squareness of the hysteresis curve. The width of the hysteresis curve shows the coercive field (H_c) while the height of the hysteresis curve represents the saturation magnetization (M_s). In Figure 4. it can be seen that the saturation magnetization magnitude increases with increasing annealing temperature. One of the reasons for this increase is the increase in crystallite size which leads to an increase in the size of the magnetic domain in the sample. The alignment of the number of atomic spins along with the applied magnetic field increases with increasing magnetic domain, which leads to an increase in saturation magnetization with an increase in crystallite size (Kumar & Kar, 2011). At lower annealing temperatures, the crystallite size becomes smaller due to structural distortion. This structural distortion occurs on the external surface which causes the surface spins to be in a disordered state and the cation coordination becomes very low, resulting in the breaking of the exchange bonds, which greatly affects the superexchange interaction. This is one of the saturation magnetization factors at higher annealing temperatures which has a greater magnitude than at lower annealing temperatures.

3.4 Photocatalyst

3.4.1 Effect of catalyst mass on photocatalyst activity

In this study, the effect of the catalyst mass $CoBi_{0.15}Fe_{1.85}O_4$ in reducing the pollutant methylene blue. The masses used were 10 mg, 20 mg, and 30 mg. The concentration of methylene blue used was 20 ppm. UV irradiation was carried out for 5 minutes.

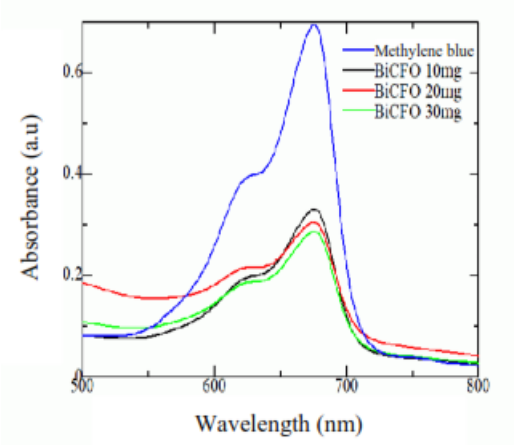

Figure 5 UV-Vis absorbance spectra of the effect of catalyst mass from a sample of bismuth cobalt ferrite at an annealing temperature of 200 ℃.

Based on Figure 5 bismuth cobalt ferrite catalyst mass greatly affects changes in absorbance magnitudes. When methylene blue reacts with bismuth cobalt ferrite and is irradiated with a UV lamp, the absorbance spectra decrease as the catalyst mass increases. This shows that bismuth cobalt ferrite catalyst works well as photocatalyst materials.

Table 1 Percentage of 20 ppm methylene blue reduction, reaction, and band gap energy for various catalyst masses.

M	Reduction (%)	$k_{reaction}$ $(\times 10^{-4})s^{-1}$	E_g (E_v)
10	54.01	25.89	1.7761
20	57.65	28.64	1.7773
30	60.11	30.63	1.7752

Table 1 presents the calculated reduction percentage of methylene blue, the kinetic reaction rate, and the energy band gap on the mass variation of the pollutant. The kinetics of the reaction rate shows the speed of the catalyst in reducing methylene blue. The reaction rate kinetics are 25.89 $\times 10^{-4}s^{-1}$, 28.64 $\times 10^{-4}s^{-1}$, 30.63 $\times 10^{-4}s^{-1}$. While the percentage reduction magnitudes are 54.01%, 57.65%, and 60.11%. It can be seen that the greater the mass of the catalyst, the faster the kinetics of the reaction rate and the greater the percentage reduction of methylene blue. These results are in accordance with previous studies (Adeleke et al., 2018). From these results, the maximum magnitude in the investigated range for reducing methylene blue is a catalyst with a mass of 30 mg. Therefore, in the next variation step using a mass of bismuth cobalt ferrite of 30 mg.

3.4.2 Effect of catalyst time on photocatalyst activity

The photocatalytic activity studies of the effect of ultraviolet irradiation time on the absorbance magnitude are shown in Figure 6. There is a decrease in the absorbance magnitude with increasing irradiation time. Holes (h^+) and electrons (e^-) are formed on the surface of the bismuth cobalt ferrite catalyst due to UV exposure. Then hydroxyl ions (OH^-), holes (h^+), electrons (e^-), and superoxide ions (O_2) react which are useful for degrading dyes from organic pollutants or methylene blue (Chaudhary et al., 2020). The increase in UV irradiation time causes the formation of more holes (h^+) and electrons (e^-). So the reaction to produce hydroxide free radicals will also increase. This causes the absorbance to decrease as the UV irradiation time increases.

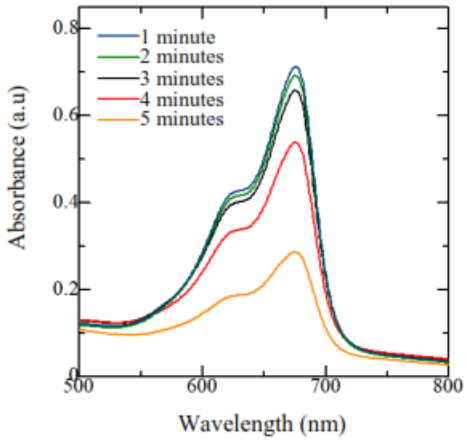

Figure 6 Photocatalytic activity studies the effect of irradiation time of bismuth cobalt ferrite samples at an annealing temperature of 200 °C.

Table 2 Percentage of 20 ppm methylene blue reduction, reaction, and band gap energy on variations in UV irradiation time.

t	Reduction (%)	$k_{reaction}$ ($\times 10^{-4}$)s^{-1}	E_g (E_v)
1	0.96	0.32	1.7763
2	12.66	4.51	1.7751
3	8.50	2.96	1.7768
4	25.14	9.65	1.7736
5	60.11	30.63	1.7752

The results of the calculation of the percentage reduction, reaction rate kinetic, and band gap energy are presented in Table 2. The percentage reduction and reaction rate kinetic does not show a certain pattern. In the percentage reduction, all-time variations showed an increase, but at 3 minutes of

UV irradiation, the percentage decreases. The decrease occurs because of the agglomeration that affects the photocatalytic surface area. A larger surface area will improve photocatalytic performance (Adeleke et al., 2018).

4. CONCLUSION

Cobalt ferrite-based nanoparticles with high purity were obtained experimentally and XRD analysis showed that the bismuth cobalt ferrite sample complies with ICDD 221086. The maximum magnitude in the investigated range of bismuth cobalt ferrite catalyst to reduce pollutants or methylene blue is 30 mg, which is 60.11%. UV irradiation treatment at 5 minutes results in the greatest reduction percentage, which is 60.11%. The results of this study indicate that cobalt ferrite-based nanoparticles have potential as photocatalyst materials. This study aims to confirm that bismuth cobalt ferrite samples can be used for photocatalyst applications. Further research can be carried out to increase the percentage degradation of bismuth cobalt ferrite samples.

REFERENCE,

Adeleke, J. T., Theivasanthi, T., Thiruppathi, M., Swaminathan, M., Akomolafe, T., & Alabi, A. B. (2018). Photocatalytic degradation of methylene blue by ZnO/NiFe 2 O 4 nanoparticles. *Applied Surface Science*, 455, 195–200.

Amer, M. A., Meaz, T. M., Mostafa, A. G., & El-Ghazally, H. F. (2015). Annealing effect on the structural and magnetic properties of the CuAl0.6Cr0.2Fe1.2O4 nano-ferrites. *Materials Research Bulletin*, 67, 207–214.

Amiri, S., & Shokrollahi, H. (2013). Magnetic and structural properties of RE doped Co-ferrite (RE=Nd, Eu, and Gd) nano-particles synthesized by co-precipitation. *Journal of Magnetism and Magnetic Materials*, 345, 18–23.

Arilasita, R., Utari, & Purnama, B. (2020). The effect of annealing on the crystalline structure of CoBi0.1Fe1.9O4 nanoparticles. *AIP Conference Proceedings*, 2296(November), 4–9.

Chaudhary, K., Shaheen, N., Zulfiqar, S., Sarwar, M. I., Suleman, M., Agboola, P. O., Shakir, I., & Warsi, M. F. (2020). Binary WO3-ZnO nanostructures supported rGO ternary nanocomposite for visible light driven photocatalytic degradation of methylene blue. *Synthetic Metals*, 269, 116526.

Gingasu, D., Diamandescu, L., Mindru, I., Marinescu, G., Culita, D. C., Calderon-Moreno, J. M., Preda, S., Bartha, C., & Patron, L. (2015). Chromium substituted cobalt ferrites by glycine-nitrates process. *Croatica Chemica Acta*, 88(4), 445–451.

Goodarz Naseri, M., Saion, E. B., Abbastabar Ahangar, H., Shaari, A. H., & Hashim, M. (2010). Simple synthesis and characterization of cobalt ferrite nanoparticles by a thermal treatment method. *Journal of Nanomaterials*, 2010, 1-8.

Hajalilou, A., Mazlan, S. A., Abbasi, M., & Lavvafi, H. (2016). Fabrication of spherical CoFe2O4 nanoparticles via sol-gel and hydrothermal methods and investigation of their magnetorheological characteristics. *RSC Advances*, 6(92), 89510–89522.

Kapoor, S., Goyal, A., Bansal, S., & Singhal, S. (2018). Emergence of bismuth substituted cobalt ferrite nanostructures as versatile candidates for the enhanced oxidative degradation of hazardous organic dyes. *New Journal of Chemistry*, 42(18), 14965-14977.

Kiran, V. S., & Sumathi, S. (2017). Comparison of catalytic activity of bismuth substituted cobalt ferrite nanoparticles synthesized by combustion and co-precipitation method. *Journal of Magnetism and Magnetic Materials*, 421, 113–119.

Kotnala, R. K., & Shah, J. (2015). *Ferrite Materials: Nano to spintronics Regime*. In Handbook of Magnetic Materials (Vol. 23). Elsevier.

Kumar, L., & Kar, M. (2011). Effect of annealing temperature and preparation condition on magnetic anisotropy in nanocrystalline cobalt ferrite. *IEEE Transactions on Magnetics*, 47(10), 3645–3648.

Labhane, P. K., Huse, V. R., Patle, L. B., Chaudhari, A. L., & Sonawane, G. H. (2015). Synthesis of Cu Doped ZnO Nanoparticles: Crystallographic, Optical, FTIR, Morphological and Photocatalytic Study. *Journal of Materials Science and Chemical Engineering*, 03(07), 39–51.

Ramli, R., Jonuarti, R., & Hartono, A. (2017). Analisis Struktur Nano Dari Lapisan Tipis Cobalt Ferrite Yang Dipreparasi Dengan Metode Sputtering. *EKSAKTA: Berkala Ilmiah Bidang MIPA*, 18(01), 46–53.

Routray, K. L., Sanyal, D., & Behera, D. (2017). Dielectric, magnetic, ferroelectric, and Mossbauer properties of bismuth substituted nanosized cobalt ferrites through glycine nitrate synthesis method. *Journal of Applied Physics*, 122(22), 224104.

Safaat, M. (2020). Potensi Logam Oksida Sebagai Fotokatalis Degradasi Plastik Di Air Laut. *Oseana*, 45(1), 40–58.

Saputro, D. E., Utari, & Purnama, B. (2019). XRD and FTIR analysis of bismuth substituted cobalt ferrite synthesized by co-precipitation method. *Journal of Physics: Conference Series*, 1153(1).

Setiadi, E. A., Shabrina, N., Budi Utami, H. R., Fahmi, N. F., Kato, T., Iwata, S., & Suharyadi, E. (2016). Sintesis Nanopartikel Cobalt Ferrite (CoFe2O4) dengan Metode Kopresipitasi dan Karakterisasi Sifat Kemagnetannya. *Indonesian Journal of Applied Physics*, 3(01), 55.

Sumathi, S., & Lakshmipriya, V. (2017). Structural, magnetic, electrical and catalytic activity of copper and bismuth co-substituted cobalt ferrite nanoparticles. *Journal of Materials Science: Materials in Electronics*, 28(3), 2795–2802.

Sundararajan, M., John Kennedy, L., Nithya, P., Judith Vijaya, J., & Bououdina, M. (2017). Visible light driven photocatalytic degradation of rhodamine B using Mg doped cobalt ferrite spinel nanoparticles synthesized by microwave combustion method. *Journal of Physics and Chemistry of Solids*, 108, 61–75.

Syam, B., & Hendri, W. (2014). Sintesis Film Tungsten Oksida (Wo3) dengan Penambahan Metal Co-katalis Besi (Fe) dan Aplikasinya pada Peningkatan Aktivitas Fotokatalitik Degradasi Zat Warna Methylene Blue Menggunakan Cahaya Matahari. *Youngster Physics Journal*, 3(1), 15–24.

Zhang, Y., Yang, Z., Yin, D., Liu, Y., Fei, C., Xiong, R., Shi, J., & Yan, G. (2010). Composition and magnetic properties of cobalt ferrite nano-particles prepared by the co-precipitation method. *Journal of Magnetism and Magnetic Materials*, 322(21), 3470–3475.

Zhou, L., Fu, Q., Zhou, D., Xue, F., & Tian, Y. (2015). Solvothermal synthesis of CoFe2O4 submicron compact spheres and tunable coercivity induced via lowhttp:erature thermal treatment. *Journal of Magnetism and Magnetic Materials*, 392, 22–26.